Magnetic Ordering and the Electronic Properties of the Heavy Rare-Earth Metals

R. E. WATSON

Brookhaven National Laboratory, Upton, New York*

AND

A. J. FREEMAN†

National Magnet Laboratory,‡ Massachusetts Institute of Technology, Cambridge, Massachusetts

AND

J. P. DIMMOCK

Lincoln Laboratory,§ Massachusetts Institute of Technology, Lexington, Massachusetts

(Received 1 November 1967)

The magnetic perturbation of the conduction-electron bands due to the periodic (and ferromagnetic) arrays of $4f$ moments, occurring in the heavy rare-earth metals, has been estimated from nonrelativistic augmented-plane-wave energy-band results for Tm. The relationship between these perturbations, the ordering period, and other observables, such as the c-axis resistance anomalies, are inspected. Important to these considerations and to an understanding of the ordering of the $4f$ moments is the magnitude of the perturbation effects which result in sizable gaps relative to the bandwidth in the $5d$ bands, destroy large segments of Fermi surface (primarily normal to the c axis), and force appreciable redistributions of the populated conduction-electron states.

I. INTRODUCTION

THE heavy rare-earth metals, Gd through Tm, display a large diversity of magnetic orderings at low temperatures. As is well known, a number of interesting phenomena occur at the onset of this ordering, including optical and anisotropic resistance anomalies. We have previously shown that the transition-metal-like nature of the heavy rare-earth conduction bands, which are strongly hybridized $5d$–$6s$ bands, is important to the understanding of these properties.[1] In the present paper we examine the nature of the magnetic perturbation of these bands by the periodic magnetic ordering and consider the relationship between these perturbations, the $4f$ ordering itself and the observed resistance anomalies. The optical anomalies, assumed to be associated with exchange-induced gaps in the conduction bands, are employed to estimate the $4f$–$5d$ band exchange coupling. These yield results in approximate agreement with *a priori* estimates of this coupling.

Nonrelativistic augmented-plane-wave (APW) band results for Tm metal are presented and discussed in Sec. II. Particular emphasis is placed on the largely $5d$-like bands yielding the Fermi surface normal to the c axis, for it is these bands which are important to all the unusual properties of the heavy rare earths. These bands are found to be extraordinarily narrow. This fact is essential to understanding the properties of these metals, but unfortunately also results in some problems since details of the bands which are of physical significance are within the uncertainties of current band estimates—both nonrelativistic and relativistic.

The energy-band results for Tm are utilized in subsequent sections for all the rare-earth metals, Gd through Tm. In doing this, we emphasize the common features of the bands of all these metals, since details, such as small differences in band character which do arise when going from Gd to Tm, lie within the uncertainties of all present band calculations. This is associated, in part, with the narrowness of the important $5d$ bands. As emphasized in Sec. II, a detailed quantitative treatment of the problems at hand requires nonmagnetic band results which are one or more orders of magnitude more accurate than those currently available. Following this, the general nature and magnitude of the $4f$ conduction-electron exchange coupling is considered for the spiral arrays of interest. The perturbation of the $5d$ bands due to the ordered $4f$ moments is then inspected. The perturbations introduce gaps in the bands largely at or near the Fermi-surface sections normal to the hexagonal axis, thereby destroying or perturbing large segments of that surface. The effect of these perturbations is shown to be large and the gaps introduced approach the important bandwidths. This has many implications. For example, states well away from the Fermi energy contribute significantly to the $4f$–$4f$ exchange energy and, in turn, are a contributing factor in determining the nature of the magnetic spiral. The relation of the $4f$ moment ordering to the band structure, the local-moment–conduction-electron exchange, and to other terms, such as anisotropic crystal-field terms, is discussed in the final section of the paper.

* Supported by the U.S. Atomic Energy Commission.

† Permanent address: Department of Physics, Northwestern University, Evanston, Ill.

‡ Supported by the U.S. Air Force Office of Scientific Research.

§ Operated with support from the U.S. Air Force.

[1] A. J. Freeman, J. O. Dimmock, and R. E. Watson, Phys. Rev. Letters **16**, 94 (1966).

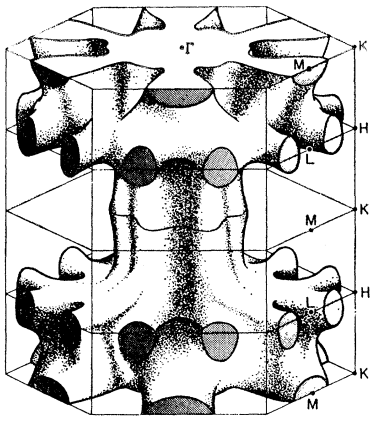

FERMI HOLE SURFACE FOR THULIUM METAL

FIG. 1. The double-zone representation of the Fermi surface of nonmagnetic Tm metal as obtained from a nonrelativistic APW band calculation [after Freeman, Dimmock, and Watson (Ref. 1)].

II. THE FERMI SURFACE AND *d* BANDS OF Tm

The Fermi surface of Tm, which has been reported by us previously, is shown in Fig. 1. Cross sections of this Fermi surface appear in Fig. 2. The Fermi-hole surface, plotted in the double zone scheme, consists of a trunk, contributed by bands of largely *s–p* character, and arms in the vicinity of the *ALH* plane, which arise from bands of largely *d* character. The trunk provides the Fermi surface parallel to the *c* axis while the arms are responsible for that perpendicular to it. The energy-versus-*k* plots of Fig. 3 show the relatively steep *s–p* band contributing to the trunk.

The resistance anomalies due to the magnetic ordering of the rare earths occur in the *c*-axis direction. We therefore wish to inspect in some detail the bands contributing to the Fermi surface normal to that direction. Energy-versus-*k* plots for **k** running parallel to the *c* axis are shown in Fig. 4 for lines *A* through *E*, indicated in Fig. 2. Note from Fig. 2 that the lines cross nearly normal to the Fermi-surface cross section. The bands in Fig. 4 are unusually flat. In some of the plots the pair of bands, which in all cases is the third and fourth bands intersecting the Fermi energy, have a total width of only about 0.5 eV, which is of the order of the spin-orbit splitting. This implies large effective masses, substantial contributions to the density of states $N(E)$, and large effects due to the exchange field perturbations which introduce magnetic band gaps of the order of 0.1 to 0.6 eV. These perturbations will be of primary interest to us in the remainder of this paper.

The flat character of the *d* bands makes it difficult to determine the details of the Fermi surface normal to *c*. For example, raising the bands shown in Fig. 4(E) by ~0.2 Ry at the point *L* causes the pairs of arms of Fig. 1 to merge into single larger arms. Such a shift is within the uncertainties of the band calculations. A number of factors, quite aside from numerical accuracy, contribute to these uncertainties and several deserve mention here. A traditional problem associated with APW calculations for transition metals is the choice of atomic starting potential (in particular its effect on the relative placement of the *s* and *d* bands). Gd band calculations[2] employing various nonrelativistic potentials suggest that this uncertainty is of the order of ~0.02 Ry in the placement of one band with respect to another. The approximate exchange potential[3–5] employed in such band calculations introduces another source of uncertainty. Comparing results obtained[2] with the Slater[3] and the Gaspar[4] approximations suggests the uncertainty from this source to be ~0.04 Ry. Finally, the present results are nonrelativistic. Comparison of these with the relativistic results of Keeton and Loucks[6] indicates that the differences are within the uncertainties of either calculation.

Details of the Fermi surface of a nonmagnetic rare-earth metal are uncertain due to these inaccuracies in current band calculations. We nevertheless expect that the essential features of Figs. 1 and 2 are correct; namely, the existence of "*s–p*" band trunk and the *d* band arms in the vicinity of the *ALH* plane. The arms may have different shape from that shown, but the process of filling the bands with three electrons per atom inevitably causes E_F to intersect those bands giving rise to the arms. We will employ the bands (A through D) of Fig. 4 when endeavoring to relate the band structure to some of the electrical and magnetic properties of the magnetized metals. We will discover that the exchange perturbation of the bands, due to an ordered array of 4*f* moments, is so severe that one can obtain only qualitative information from a description starting with the nonmagnetic band structure. For this reason, uncertainties in details of the present bands and their associated Fermi surface will not be too important to us. Significantly improved knowledge of these details awaits assistance from experiment.

III. MAGNETIC STRUCTURES AND THE 4*f* CONDUCTION-ELECTRON EXCHANGE COUPLING IN THE HEAVY RARE EARTHS

Gd is ferromagnetic whereas the heavier rare earths, Tb through Tm, take on the spiral spin structures displayed in Fig. 5 on going through their Néel points.

[2] J. O. Dimmock, A. J. Freeman and R. E. Watson, in *Proceedings of the International Colloquium on Optical Properties and Electronic Structure of Metals and Alloys*, edited by F. Abeles (North-Holland Publishing Co., Amsterdam, 1966), p. 237; J. O. Dimmock and A. J. Freeman, Phys. Rev. Letters **13**, 750 (1964); and (to be published).

[3] J. C. Slater, Phys. Rev. **81**, 385 (1951).

[4] R. Gaspar, Acta Phys. Hung. **3**, 263 (1954); W. Kohn and L. J. Sham, Phys. Rev. **140**, A1133 (1965).

[5] J. C. Slater, Quarterly Progress Report No. 58, Solid-State and Molecular Theory Group, M.I.T., 1965 (unpublished).

[6] S. C. Keeton and T. L. Loucks (to be published).

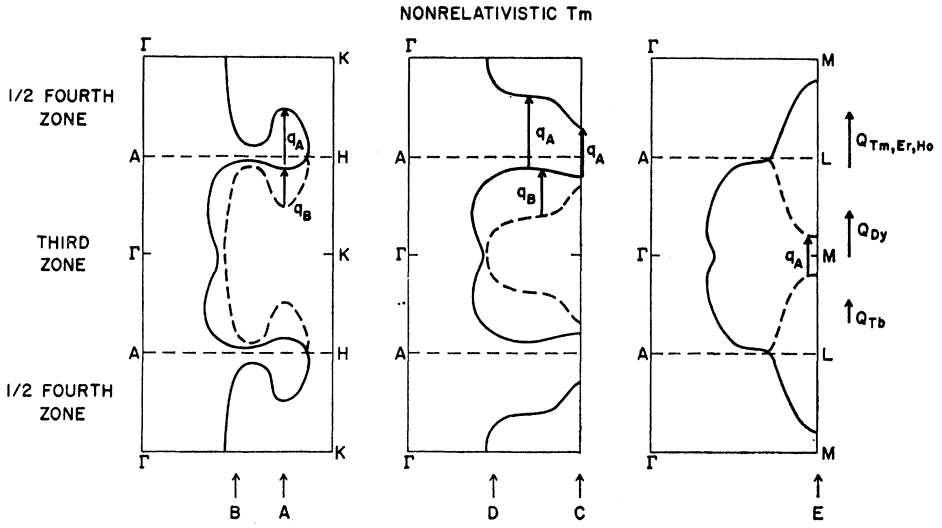

FIG. 2. Cross sections of the Fermi surface displayed in Fig. 1. Dashed curves show the fourth-zone Fermi surface folded into the third zone. The q_A and q_B vectors indicate typical Fermi-surface calipers as is discussed in the text.

Further lowering of temperature is accompanied by (1) increasing spiral wave length and (2) further magnetic transitions, generally to spirals with ferromagnetic components, additional higher harmonics, or to pure ferromagnetic states.[7] We will be primarily interested in the effect of magnetic ordering on the band structure and Fermi surface at the onset of magnetic ordering and will concentrate on the spirals displayed in Fig. 5, using Tm and Ho as examples of the two types. The spin ordering is given by the average spin values of the types:

$$\text{Tm type:}\quad \langle S_n^z\rangle = SM\cos(\mathbf{Q}\cdot\mathbf{R}_n+\phi), \qquad (1a)$$

where Q is parallel to the hexagonal c axis (taken to be the z axis) so that (1a) gives a longitudinal wave.

$$\text{Ho type:}\quad \langle S_n^x\rangle = SM'\cos\mathbf{Q}\cdot\mathbf{R}_n,$$
$$\langle S_n^y\rangle = SM'\sin\mathbf{Q}\cdot\mathbf{R}_n, \qquad (1b)$$

which gives a spiral structure, with the moments in the hexagonal planes. Here M and M', where $0<M$, $M'<1$, are temperature-dependent factors associated with the sublattice magnetization.

We are interested in the effect of these spin structures on the conduction bands and for this purpose it is con-

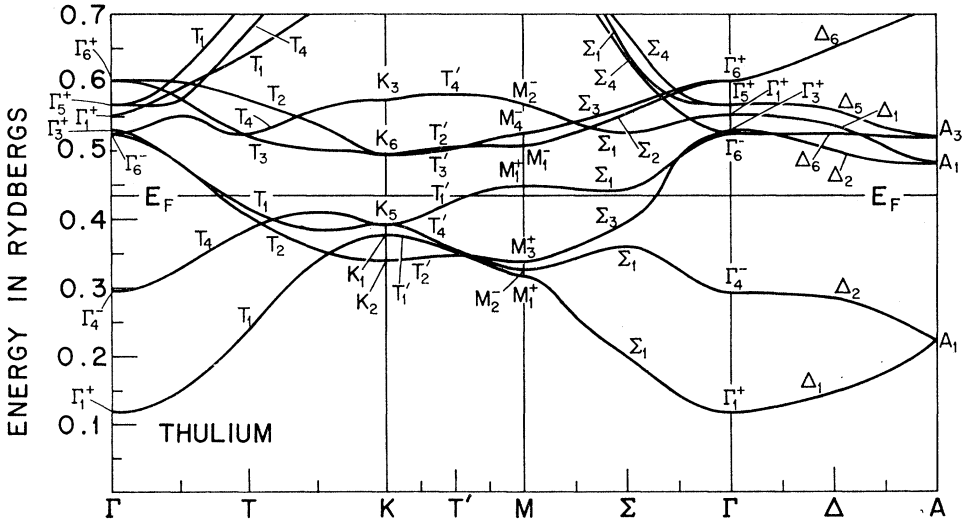

FIG. 3. Energy versus k plotted along high symmetry lines for nonmagnetic Tm.

[7] For a review of the magnetic ordering of the rare earths, see, for example, H. R. Child, Oak Ridge National Laboratory Report No. TM 1063, 1965 (unpublished); or R. J. Elliott, in *Magnetism*, edited by G. Rado and H. Suhl (Academic Press Inc., New York, 1965), Vol. IIA.

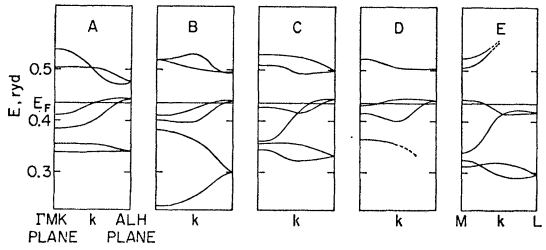

FIG. 4. Energy versus k, for nonmagnetic Tm, plotted for the c-axis lines A through E indicated in Fig. 2. For all cross sections but D, the lower two bands are displayed. Similarly, nearest lying higher bands are shown, except in E.

venient to use the exchange Hamiltonian

$$\mathcal{H}_{\mathbf{k},\mathbf{k}'} = -(2/N)\sum_n \mathcal{J}(\mathbf{k},\mathbf{k}')\,\exp[i(\mathbf{k}-\mathbf{k})\cdot\mathbf{R}_n]\mathbf{S}_n\cdot\boldsymbol{\sigma} \quad (2)$$

for the coupling between Bloch orbitals with wave vectors $\mathbf{k}$ and $\mathbf{k}'$. Here S_n is the $4f$ spin at the nth atom at position R_n. N is the number of lattice sites and $\boldsymbol{\sigma}$ is the conduction-electron spin operator. The exchange integral $\mathcal{J}$ is

$$\mathcal{J}(\mathbf{k},\mathbf{k}') \equiv N\left\langle \iint \phi_{\mathbf{k}}^*(\mathbf{r}_1)\psi_f(\mathbf{r}_1)r_{12}^{-1}\psi_f^*(\mathbf{r}_2)\phi_{\mathbf{k}'}(\mathbf{r}_2)\,d\tau_1 d\tau_2 \right\rangle, \quad (3)$$

where the ϕ's are conduction-electron orbitals, the ψ's are local moment orbitals, both situated at $R_n=0$, and the integral is averaged over the ψ's making up the local moment. The factor N makes $\mathcal{J}$ of the order of an atomic exchange integral. Following standard practice, $\mathcal{J}$ will be assumed a function of the scalar difference $|\mathbf{k}-\mathbf{k}'| = q$. At best this is a crude approximation[8] to the $\mathbf{k}$ and $\mathbf{k}'$ dependence of Eq. (3) but a more precise accounting is beyond our current purposes.

The occurrence of a ferromagnetic array of local moments induces an exchange splitting of the conduction bands

$$\Delta_{\text{ferro}} = SM\mathcal{J}(0), \quad (4)$$

where S is the expectation value of the local spin moment and $\mathcal{J}(0)$ is the diagonal ($\mathbf{k}=\mathbf{k}'$) matrix element. The assumption of a $\mathcal{J}$ which is a function of only $|\mathbf{k}-\mathbf{k}'|$ implies a simple rigid, k-independent, exchange splitting of spin parallel and spin antiparallel bands when the $4f$ moments are ordered ferromagnetically.

Band gaps arise instead of the rigid splitting if the local spin moments order in either of the spirals of Fig. 5. Inserting either of the spiral structures into Eq. (2) yields off-diagonal exchange matrix elements between Bloch states for $\mathbf{k}-\mathbf{k}' = \pm\mathbf{Q}+\boldsymbol{\tau}$, $\boldsymbol{\tau}$ being any reciprocal-lattice vector. These matrix elements arise between states of like spin for the Tm spiral and between states $\mathbf{k}$ of spin down and $\mathbf{k}+\mathbf{Q}+\boldsymbol{\tau}$ of spin up for the Ho spiral.[9] Band gaps occur when $\mathbf{Q}+\boldsymbol{\tau}$ connects a degenerate pair of band states. These gaps are

$$\Delta_{\text{Tm}} = MS\mathcal{J}(\mathbf{Q}+\boldsymbol{\tau})\,|\,F(\boldsymbol{\tau})\,| \quad (5a)$$

and

$$\Delta_{\text{Ho}} = 2M'S\mathcal{J}(\mathbf{Q}+\boldsymbol{\tau})\,|\,F(\boldsymbol{\tau})\,|, \quad (5b)$$

where $F(\boldsymbol{\tau})$ is the structure factor

$$F(\boldsymbol{\tau}) = (1/n)\sum_{i=1} \exp(i\mathbf{R}_i\cdot\boldsymbol{\tau}) \quad (6)$$

summed over n atomic sites in a unit cell in real space. The presence[9] of $F(\boldsymbol{\tau})$ causes the mixing and associated gaps to vanish for certain values of $\boldsymbol{\tau}$.

The bands intersecting the Fermi surface lie, in the extended zone scheme, in the 3rd and 4th Brillouin zones and $\tau=0$ couplings may occur within a band in a single zone and between bands across the (001) boundary between zones. A number of such inter- and intraband Q vectors, designated as q_A, are shown in Fig. 2. The case of $\boldsymbol{\tau}=(001)$ is also of interest since it includes interband terms such as the q_B of Fig. 2. The structure factor is zero for $\tau=(001)$, indicating that this mixing is zero in first approximation. Some mixing and associated gaps will occur because spin-orbit coupling, which we

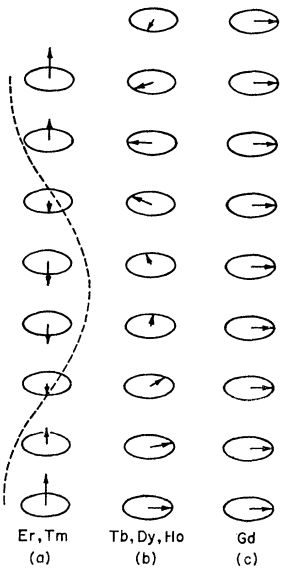

FIG. 5. The $4f$ spin arrangements of the rare-earth metals formed at the onset of magnetic ordering.

[8] R. E. Watson and A. J. Freeman, Phys. Rev. **152**, 566 (1966); R. E. Watson, in *Hyperfine Interactions*, edited by A. J. Freeman and R. B. Frankel (Academic Press Inc., New York, 1967).

[9] R. J. Elliott and F. A. Wedgewood, Proc. Phys. Soc. (London) **81**, 846 (1963); **84**, 63 (1964).

have neglected in the APW calculations, will mix the bands and render Eq. (6) invalid. We nevertheless expect such q_B gaps to be smaller than the $\tau=0$, q_A gaps. Spin-orbit mixing will also cause initially zero-valued Ho spiral-matrix elements to take on small nonzero values. For bands to mix in such a way as to lower the energy of the system in first order, their slopes at E_f must be opposite in sign, in which case the mixing takes place between occupied and unoccupied states.[10] For the bands shown in Fig. 4, the q_A vectors of Fig. 2 meet this criterion whereas the q_B vectors do not. In the sections which follow, the q_B mixing will be neglected.

In order to estimate the effect on the bands of the spiral perturbations, one requires a knowledge of the exchange coupling $\mathcal{J}(Q)$. The value $\mathcal{J}(0)$ is readily estimated utilizing the conduction-electron moment $\Delta\mu$, observed in ferromagnetic Gd. Assuming no conduction-electron–conduction-electron enhancement of the response, $\Delta\mu$ is given by

$$\Delta\mu=\tfrac{1}{4}g\mu_B N(E_F)\Delta_{\text{ferro}}. \tag{7}$$

For Gd the total moment is observed to be 7.55 μ_B per atom,[11] of which 0.55 μ_B is considered to be due to conduction-electron polarization. Taking the calculated value[2] of $N(E_F)=1.8$ electrons per atom per eV, Eqs. (4) and (7) yield $\mathcal{J}(0)\sim 0.087$ eV, assuming $g=2$ for the conduction electrons.

Given $\mathcal{J}(0)$ for Gd and assuming the same value for the heavier rare earths Δ_{ferro} becomes proportional to S. The values obtained for the heavy rare earths are listed in Table I.[2] The moderate variation in band structure and $4f$-shell character, with varying nuclear charge Z, suggest this to be a reasonable first approximation. As has been already indicated,[2] there is a remarkable agreement between the values obtained and the energies of the optical anomalies observed at 0.44 eV for Dy[12] and 0.35 eV in Ho,[13] which have appeared with the onset of magnetic ordering. Dy and Ho order in the Ho-type spiral displayed in Fig. 5(b) with the associated energy gap given by Eq. (5b). The exchange coupling is therefore associated with a nonzero Q. If the above arguments are correct, Eq. (5b) taken with the observed anomalies yields

$$\mathcal{J}(Q)_{\text{Ho}}\sim\mathcal{J}(Q)_{\text{Dy}}\sim\mathcal{J}(0)_{\text{Gd}}. \tag{8}$$

Estimates of the coupling between the $4f$ shell and orthogonalized plane waves yield[8] $\mathcal{J}(Q)<\mathcal{J}(0)$. The present observations suggest a much weaker q dependence for the coupling between the $4f$ shell and the $5d$ bands involved here.

An interesting feature of the optical results obtained by Cooper and Redington[12] is that the application of a magnetic field to Dy, sufficient to force the $4f$ moments out of the spiral and into a ferromagnetic array, resulted in "no measurable change" in the anomaly. Equations (4), (5b), and (8) suggest that the position (but not necessarily the shape) of the anomaly should stay fixed.

The above discussion has assumed that the exchange coupling remains constant as one moves across the heavy rare-earth series. In concluding this section, it should be noted that the experimentally observed Néel temperatures crudely support this assumption.[14] For any given type of spiral one would expect, using a constant $\mathcal{J}$, that

$$T_N\propto(g-1)^2J(J+1), \tag{9}$$

where J is the total angular momentum. There is a distinct suggestion that $\mathcal{J}$ increases somewhat with increasing Z. These matters will be considered in a future paper.

TABLE I. Observed spiral Δ's compared with the Δ_{ferro} for the heavy rare-earth metals as predicted by Eqs. (4) and (7), employing the observed $\Delta\mu$ for Gd.

	S	Δ_{ferro} (eV)	Δ
Gd	$\frac{7}{2}$	0.61	
Tb	3	0.52	
Dy	$\frac{5}{2}$	0.44	0.44
Ho	2	0.35	0.35
Er	$\frac{3}{2}$	0.26	
Tm	1	0.17	

IV. EXCHANGE PERTURBED BANDS IN Tm

As already noted, the Tm spiral [Eq. (1a)] introduces exchange coupling between a state $\mathbf{k}$ and states $\mathbf{k}\pm\mathbf{Q}$ of like spin. Of course a state $\mathbf{k}+\mathbf{Q}$ will mix in turn with $\mathbf{k}+2\mathbf{Q}$, and so on. Computational matters are simplified by the fact that the Tm spiral is commensurate with the lattice, with a Q which is one-seventh the double-zone c-axis dimension (see Q_{Tm} in Fig. 2). Then, since $\mathbf{k}+7\mathbf{Q}$ has returned to $\mathbf{k}$, we may abandon perturbation theory and explicitly diagonalize a 7×7 matrix for a given choice of $\mathbf{k}$, i.e., for states $\mathbf{k}, \mathbf{k}+\mathbf{Q}, \mathbf{k}+2\mathbf{Q}\cdots\mathbf{k}+6\mathbf{Q}$. Once one has the energies of the states involved, obtained from a nonmagnetized metal band calculation, and has assumed a value for the exchange constant $\mathcal{J}(Q)$, the process is trivial to carry out. Inspection of the resulting eigenvectors normally shows that one k component, of one band, dominates. Plotting the energies of the perturbed bands as a function of these dominant k components, one obtains

[10] M. Lomer, discussions at U.S.-Japan Science Seminar, Williamstown, Mass., 1967 (unpublished).
[11] H. Nigh, S. Legvold, and F. H. Spedding, Phys. Rev. **132**, 1092 (1963).
[12] B. R. Cooper and R. W. Redington, Phys. Rev. Letters **14**, 1066 (1965).
[13] C. C. Schüler, Phys. Letters **12**, 84 (1964).
[14] For example, see Ref. 7, or P. G. de Gennes, Compt. Rend. **247**, 1836 (1958).

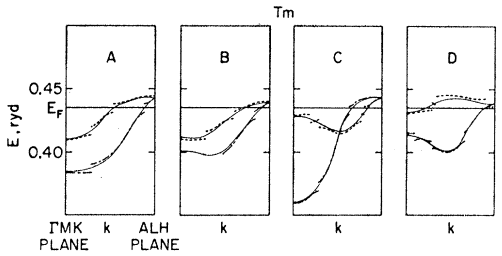

FIG. 6. The exchange perturbation induced by the Tm 4*f* spiral in conduction-electron bands A through D of Fig. 4. Because of uncertainties primarily in the nonmagnetic bands, these results should be considered to be only qualitative.

the results seen in Fig. 6 (for sections A through D of Fig. 4). This identification was straightforward with the exception of the lower part of the lower band in B, where violent mixing was associated with three close-lying gaps. This identification has not been attempted, and this region of the band is not plotted. The results reported in this section (and the next also) should be viewed as representing only schematically the actual effects of magnetic ordering on the energy bands.

Gaps of up to 0.085 eV have appeared at, or close to, all but one intersection of the bands with the Fermi energy and this band, in D, would have such a gap if $\tau=(001)$ mixing has been included. We have not calculated the shift in E_F due to the band perturbations, but we expect the shift to be small compared to the uncertainties in placement of the nonmagnetic bands with respect to one another and with the placement of the nonmagnetic E_F.

Even in the presence of the magnetic perturbation, one will still have a volume of hole states in k space much like that plotted in Fig. 1 but the volume is now bounded by energy gaps, as well as by Fermi-surface segments. The gaps will largely replace Fermi-surface sections normal to the c axis since the Fermi surface associated with the flat d bands is most severely perturbed while the "s-p" band Fermi surface of the hollow trunk, involving steeper bands, is rather less perturbed. The effect of this is to produce[1] resistance anomalies parallel, but not perpendicular, to the c axis, as are seen experimentally.

Before leaving this section, we must emphasize that details, such as whether the gaps do or do not hit E_F in particular band section A, B, or C, are within the uncertainty in position of bands with respect to one another and to E_F. However, the correlation between spiral length and Fermi-surface calipers is not accidental and such gaps will occur at or near E_F.

V. EXCHANGE PERTURBED BANDS FOR THE Ho SPIRAL STRUCTURE

The Ho spiral [Eq. (1b)] exchange couples Bloch states of wave vector k and spin $\downarrow$ *only* with states $\mathbf{k}+\mathbf{Q}$ and spin $\uparrow$. Inclusion of spin-orbit coupling, however, mixes the spin character, causing the states of wave vector $\mathbf{k}$ to be coupled with both states $\mathbf{k}+\mathbf{Q}$ and this in turn with $\mathbf{k}+2\mathbf{Q}$, etc. This leads to chains of coupled states of the type seen for Tm. These are, however, more weakly coupled, since this process depends on the presence of both spin components in a given Bloch state. In the absence of spin-orbit coupling and q_B mixing, the problem reduces to solving a series of 2×2 secular equations resulting in states of predominantly one spin (and $\mathbf{k}$ value) or the other (and $\mathbf{k}+\mathbf{Q}$). Results have been obtained by perturbing the nonmagnetic bands of Fig. 4 (which are probably a good approximation to the energy bands for Ho) with a spiral of the same Q as was used in the preceding section and a $\mathcal{J}(Q)=\mathcal{J}(0)$ for gadolinium. Results for states of predominantly one spin α and the other β appear in Fig. 7. It should be noted that, from symmetry, the α spin bands would be appropriate to β spin, and vice versa if either the screw sense of the spiral was reversed or if the bands were to be plotted in the *minus* $\mathbf{k}$ direction rather than the plus $\mathbf{k}$ direction. The α bands connect continuously with the β bands across both the ΓMK and ALH planes.

The band gaps of 0.34 eV match the observed optical anomaly in Ho and represent a large perturbation of the bands. However, it should be remembered that Ho has the smallest spin, hence the smallest gap, among the rare earths which order in this spiral. On going from Ho to Tb, the gap increases by 50%. Because of the increase in gap size over that for Tm, a significant number of Fermi energy intersections will be severed and the c-axis resistivity is again appreciably raised. The *increasing size* of the gaps implies (1) the destruction of large sections of the Fermi surface and (2) that Bloch states, lying increasingly far from the nonmagnetic Fermi surface, take an active role in the magnetic ordering. This matter will be of interest to us in the section which follows.

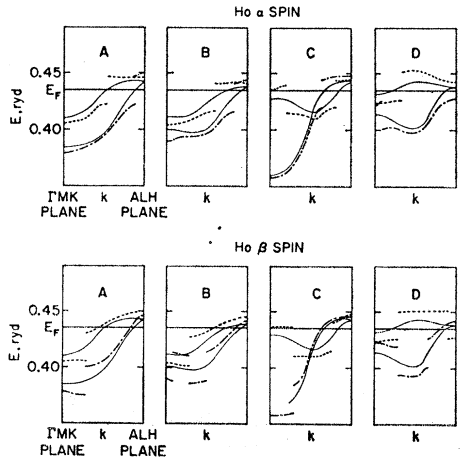

FIG. 7. The exchange perturbation, due to the Ho 4*f* spiral, of bands A through D. Results are shown separately for bands of predominantly α and β spin character. As with the Tm spiral perturbations, these results must be considered to be only qualitative.

VI. MAGNETIC ORDERING OF THE HEAVY RARE-EARTH METALS

The $4f$ moment–conduction-electron exchange interaction has been seen to severely perturb the conduction bands primarily through the introduction of several large energy gaps. When E_F falls in *or near* one of these gaps, the energy of the system is stabilized since occupied Bloch states then have their energy lowered while unoccupied states have theirs raised. (The trace of the spiral exchange energy is, of course, zero.) While we believe this stabilization energy to be essential to the temperature[9] and atomic-number dependence of the spiral Q vectors (and of tendencies to ferromagnetism), additional factors are important to the actual form a spiral takes.

Among other things, the $4f$ moments, being highly localized, interact indirectly via the perturbed conduction bands (and, to a less extent via the perturbed outer $5s$ and $5p$ shells of the ion "core"). In simple Ruderman-Kittel-Kasuya-Yosida theory[8,15–17] the exchange constant coupling two local moments, separated by R_{12}, via the conduction-electron polarization, is given by[16]

$$J(R_{12}) \sim \int d\mathbf{q} \mid \mathcal{J}(q) \mid^2 \chi(q) \exp(i\mathbf{q}\cdot\mathbf{R}_{12}), \quad (10)$$

where $\chi(q)$ is the familiar susceptibility function. Treated in greater detail the coupling between adjacent aspherical $4f$ moments involves anisotropic exchange[18] coupling. Such effects are "multimoment" in the sense that any one moment interacts anisotropically with the "effective field" due to the others. Secondly, there is the electrostatic crystal-field interaction of a $4f$ orbital moment, and, in turn, the spin moment with its environment which, unlike above, is a single-moment property in the sense that the anisotropy does not depend on the behavior of adjacent moments.[19]

Given the type of spiral order, the magnitude of the experimental Q vectors for the heavier elements correlates well with the set of c-axis Fermi-surface calipers as seen in Fig. 2. The tendency to shorter Q vectors and ultimately to ferromagnetism, as one lowers temperature and/or goes to lighter elements, is in part associated with the increasing magnitude of the energy-band perturbations associated with these two trends. One observation must be made when asserting this view. In the immediate vicinity of the Néel point, the average spin moment associated with a single site in the spiral, and in turn the spiral exchange perturbation, is small and neglecting spin-disorder scattering, one should expect Q to correlate well with Fermi-surface dimensions. Experimental results[20] for Tb indicate that this metal maintains its small Q into this temperature region. This suggests a real difference in Fermi-surface details as one goes from the heavier rare earths to Tb (and Gd). As stated earlier, our various calculations for Tm and Gd (with varying potentials) suggest that these details are within the uncertainties of the calculations: Keeton and Loucks believe[6] they have detected the Fermi-surface feature responsible for this. The strength of the exchange perturbations is, as we have demonstrated, nevertheless exceedingly important. A ferromagnetic Gd exchange gap of $\sim$0.61 eV implies that at low temperatures the bands for electrons with spin parallel to the $4f$ shell moments will be depressed to the point that the 3rd and 4th band segments plotted in Fig. 4 will be entirely under E_F.[21] This implies that c-axis conduction electrons will be primarily of spin-antiparallel character. Of more immediate concern here is the suggestion that ferromagnetism may arise when the exchange perturbation is strong enough to destroy the spin-parallel Fermi-surface arms, making it advantageous to do this rather than riding a strong Q-dependent perturbation. We believe that the violent, nonperturbative character of local-moment–conduction-electron exchange effects and Fermi-surface character are essential factors of heavy rare-earth behavior both in their effect on spiral lengths and on the tendency to ferromagnetism.

ACKNOWLEDGMENTS

We wish to thank Mrs. A. Furdyna and Miss E. Wolfson for their contributions in obtaining the unperturbed and perturbed band results, respectively. Conversations with and/or communications from R. J. Elliott, T. L. Loucks, A. R. MacIntosh, H. Bjerrum Møller, S. J. Pickart, and G. Shirane are appreciated.

[15] M. A. Ruderman and C. Kittel, Phys. Rev. **96,** 99 (1954); K. Yosida, *ibid.* **106,** 893 (1957).

[16] T. Kasuya, Progr. Theoret. Phys. (Kyoto) **16,** 45 (1956).

[17] See also, P. A. Wolff, Phys. Rev. **129,** 84 (1963); B. Giovannini, M. Peter, and J. R. Schrieffer, Phys. Rev. Letters **12,** 736 (1964); T. Moriya, Progr. Theoret. Phys. (Kyoto) **34,** 329 (1965).

[18] T. A. Kaplan and D. H. Lyons, Phys. Rev. **129,** 2072 (1963); F. Specht, Phys. Rev. **162,** 389 (1967).

[19] Neutron diffraction studies of the alloys cast light on the relative roles of these single and multimoment effects. Pickart and Shirane [J. Appl. Phys. **37,** 1032 (1966); and (unpublished)] have studied Ho_xEr_{1-x} and Dy_xEr_{1-x} alloy systems (cases where one constituent takes on the Ho, the other the Tm, spiral when a pure metal) and their results show both types of moments taking on common spiral behavior. This would suggest that multimoment anisotropies dominate. Koehler, on the other hand, has reported [Fifth Rare-Earth Research Conference, Ames, Iowa, 1964 (unpublished)] alloy results, for constituents further apart in the rare-earth row (Tb and Tm), where each type tends to go into its own (and differing) type of ordering. From all of this it appears that both multi- and single moment anisotropies are important, with perhaps the former dominating if the moments are not too different.

[20] For example, see D. E. Hegland, S. Legvold, and F. H. Spedding, Phys. Rev. **131,** 158 (1963).

[21] The rigid-band splitting involves lowering spin-parallel and raising spin-antiparallel bands by $\sim$0.3 eV with respect to E_F.